Please cite the Published Version

Additional Information: This is an Author Accepted Manuscript of an article published in Ocean Engineering, by Elsevier.

Evaluation of a GNSS for Wave Measurement and Directional Wave Spectrum Analysis

Hanbin Gu[1] Xiaoan Zhu[1] Rui Shan[2] Jun Zang[3] Ling Qian[4] Pengzhi Lin[5]

1. Institute of Ocean Engineering/School of Civil and Environmental Engineering, Ningbo University, Ningbo 315211, China；

2. Qingdao Institute of Marine Geology，CGS，Qingdao 266237，China;

3. University of Bath, BA2 7AY, UK;

4. Manchester Metropolitan University, M156BH, UK

5. Sichuan University, Chengdu, Sichuan, China, 610065 cvelinpz@126.com

Abstract

Wave buoys are important devices to monitor and analyze wave data for ocean and coastal engineering. A GNSS wave buoy is briefly introduced in the paper, which has high resolution to measure the buoy motion by vertical, north-south and west-east displacements and independent velocities in above three directions. Based on the displacements and velocities, statistical results, frequency spectra and directional spectra are analyzed, and results based on the displacements are compared with that from Waverider with a distance less than 6m deployed in the special sea water with the GNSS buoy. Wave profiles comparison show that GNSS buoy presented slightly large significant wave height and mean wave height due to its high sampling frequency, and resulted in smaller mean wave period than that from Waverider. Statisticaly, between the analyzing result of the GNSS and wave rider, the maximum error of wave height is about 5.5%; and the maximum difference of wave period is about 0.5s, when sampling frequency is similar. The energy spectra were basically consistent from these two devices. The peaks of directional spectra were similar but the spreading angle was smaller from GNSS. Results mean the GNSS device presents almost similar wave information to that from Waverider.

Keywords: GNSS, wave buoy, directional wave spectrum, frequency wave spectrum, parametric method, directional function

1 Introduction

Waves are important hydrodynamic factor in ocean, which induced by wind in local or outside of a region. Normally, wave period is from a few seconds to more than ten seconds, and the wave height is from tens of centimeters to more than ten meters. Waves often do harm to ocean structure, coastal protection, navigational ship etc. Or supply huge energy to be utilized. Therefore, wave measuring and analyzing are significant for safety of marine facilities and utility of ocean energy.

At present, lots of approaches to measuring ocean waves have been brought up. Wave gauge of capacitance or resistive wire probe (Antonov and Sadovskiy, 2007; Smolov and Rozvadovskiy, 2020) is a manner in the nearshore region, which needs a platform to support the probe, the cost of the manner is high, and the platform may have interference to wave status. Pressure transducers (Bishop and Donelan, 1987) are set on ocean bottom to measure waves, which automatically filter the wave detail on water free surface. Stereo photo surveying (Ardhuin et al. 2010) also needs a platform to support the instrument, in which the identification of air and water interface is a crucial factor for wave monitoring. Aircraft laser

altimeters (Sun et al. 2005) can be used to measure ocean waves, the manner is affected by weather, especially a tempestuous ocean status may occur extreme wave that cannot be monitored by the manner. But extreme wave is very important to ocean safety. High frequency radar (Wyatt, 2019) is applied to measure ocean wave, which has the similar issue to stereo photo surveying method on the identification of the interface between air and water. Another alternative manner is a real aperture observation technique from the Earth's orbit (Hauser et al. 2010), which is the optical method has the same issue as high frequency radar and stereo photo surveying.

The most common approach to measuring ocean wave is to apply a wave buoy. A wave buoy often has a relatively smaller diameter (0.4~0.9m) (Datawell Waverider, 2010) than weather buoy (1.2~12m), which is moored in a specified sea area. The earliest reference to wave buoy for directional wave measurement appeared in the internal report by Barber (1946) of the Admiralty Research Laboratory in England. The report suggested the basic principle, while the buoy became a reality in about fifteen years later reported by Longuet-Higgins et al. (1963). Since then, in-site ocean wave data had been collected by exclusively moored buoys, apart from shipborne wave recorder (Tucker, 1991). Datawell's Waverider has been the most successful device by measuring its own vertical acceleration on a gravity stabilized platform for non-directional wave observation. Its sensor has been refined to include tilt exception of vertical acceleration subsequently, which is the spherical directional Waverider at present. 30 years ago, the sensor Hippy 40 has been applied to many buoys around the world such as the NOAA discus buoys in the US. But the floating sphere of Datawell's Waverider sometimes led to the issue under transport and handling, even with extreme temperatures, although its sensors was proven to be robust, and the mechanical construction was refined. Later, lots of completely new conception to track the buoy motion have brought up. Steele and Earle (1991) and Wang et al. (1993) adopted magnetic field vector for azimuth, pitch and roll measurement. Steele et al. (1988) utilized low cost of angular rate sensors to consist of three orthogonal sensors. After arising of the compact unit to measure six degrees of freedom, small size, low weight of buoy can be used in wave measuring.

The satellite global positioning system (GPS) brought up further innovation to wave measuring buoy. Buoys are freed from utilizing their own sensors. Davies et al. (1997) and Rossouw et al. (2000) reported to utilize the phase tracking principle to measure buoy motion. However，the phase tracking is less robust than Doppler measurement to describe vector velocity of the buoy. The small sized Datawell's Waverider is based on GPS. Satellites are used in wave monitoring involved in the buoy positioning and velocity measuring. Four satellite systems (GPS, GLONASS, BDS and Galileo) supply more high solution to the buoy positioning and Doppler velocity measurement, because that satellite can be selected and combined to optimize the measurements. GNSS (Global Navigation Satellite System) conception has been widely applied to wave monitor (Zhu et al., 2020; Lin et al., 2020; Gendorn et al., 2019; Shan et al., 2019), water level measuring (Purnell et al., 2021; Yu 2015) currently. Most of the GNSS wave measuring literature focus on the principle of measurement, less present on GNSS wave analysis or directional wave spectrum.

The wave analysis consists of statistical analysis, frequency wave analysis and directional wave spectrum analysis. Longuet-Higgins et al. (1963) presented observations of the directional wave spectrum and brought up the parametric method to estimate the directional wave spectrum. The method has been developed by Borgman (1969), Panicker and Borgman (1974), and Hasselmann et al. (1980). The maximum likelihood method (MLM) (Capon, 1969) was extended to handle wave properties by Isobe et al. (1984). Hashimoto (1997) classified the parametric method and MLM into the conventional estimation method. During the late of 1970s, with in-situ observation data increased, more precise

directional wave spectrum methods were demanded. Hashimoto and Kobune (1985) brought up the maximum entropy principle method (MEP) and proven MEP to be an effective estimation tool. All previous methods estimating the directional spectrum with a limited mount data to describe wave characteristics in reality. But there are some undetermined factors, which induced the result may be not representative the real phenomena. Hashimoto (1987) developed the Bayesian directional spectrum estimation method (BDM). The BDM is time-consuming in iterative computation and there exist many unknown factors cannot be determined using only the obtained information. Hashimoto et al. (1993) developed the extended maximum entropy principle method (EMEP) which retains the advantages of the BDM and is more practical, because it can use three-quantity measurements and also yield equivalent results.

Recent years, wave buoy to measuring directional spectrum still has been made great progress. Gryazin and Gleb (2022) brought up a method to determine directional wave spectrum and applied it to wave buoy. The wave surface curvature is considered to determine the directional spectrum in the method. Gryazin and Gleb (2019) examined an algorithm to estimate the curvature of sea waves with use of wave velocity information. Gryazin et al. (2017) described results of a developed wave buoy to measuring the statistical characteristics, the device was designed for long-term measurement up to a season. Zhu et al. (2020) applied GNSS buoys to retrieve the significant wave height and dominant wave period near Qingdao coastline in China. The precise point positioning (PPP) and post-processed kinematic (PPK) techniques were used to get the absolute motion of the buoys, which present nearly identical significant wave height. Gendron et al. (2019) validated a GNSS buoy to measuring wave in a hydraulic flume by three processing strategies, namely, PPP and time relative positioning (TRP). The PPK and TRP presented best results compared to wave gauge data. Main advantages of PPP and TRP are that they do not require any reference station. A mean errors of wave period and wave height to sinusoidal wave are 0.06s and 0.8cm respectively. Shan et al. (2019) and Shan et al. (2018) introduced the GNSS buoy can be applied to measuring wave profiles adopted combined dynamic positioning technology of RTK, PPP and PPK. Gorman (2018) studied the issue of estimating a directional wave spectrum in terms of 3-dimensional displacement data recorded by a wave buoy, examined the limitations of existing methods to extend the "first five" directional moments from the data.

By review of wave buoy measuring directional spectrum and spectrum analyzing methods and recent wave buoy development trend, GNSS applied to wave buoy would supply an innovative change to enhance wave monitor technology. Currently GNSS buoys developers only applied the technology to obtain wave profiles and did some simple statistical analysis. Based on their measuring data a systematic directional wave analyzing method need to be done, and how about the accuracy of the wave analysis by the technique. To make this clear, a GNSS buoy is designed, in which position and velocity in the vertical direction and west-east north-south direction are independently measured; based on the data, statical wave analysis, frequency spectrum and wave directional spectrum are presented and compared with Waverider data in the same condition. In the paper, an in-house software for wave analysis is coded and compared the GNSS results to that by Waverider. The first section an introduction is presented. In the next section the GNSS instrument, its measuring theory and in-site wave data observation are briefly introduced. In the following section, wave profile and wave data are analyzed and compared with that by Waverider. In section 4, the methods of frequency spectra and directional spectra are introduced, and the directional function is discussed to keep its natural properties. Directional wave spectra analysis for data obtained by the two instruments are presented in section 5. Finally, some conclusions are listed in section 6.

2 GNSS theorem

2.1 GNSS instrument brief introduction

A GNSS buoy is designed and is composed of one main float and three auxiliary floats, all floats cylindrical, and three auxiliary floats are equidistant 120^0 from each other. The diameter of the main float is 0.5m and that of the three auxiliary ones 0.35m. A top structure is supported by the floats. At the zenith of the structure receiving GNSS antenna is set up, the receiver of Trimble Netr9 is installed in the main float seeing Fig.1. The height of the buoy above still water level is 0.5m, its draft is 0.35m and the total weight of the GNSS buoy is 50kg. During its working, the sampling frequency is 5Hz. High precision position and moving velocity of the buoy can be measured by GNSS. Merits of the GNSS buoy is that its measured velocities are independent of its measured positions, so that wave directional function can be established by more variables. The specific design is to keep GNSS sensor always higher than water free surface, because that if the sensor submerged into water, its signal would be blocked.

2.2 GNSS theorem

GNSS is an integrated global position and navigation satellite system, in which GPS、GLONASS、BDS and Galilleo satellites are selected to optimize combination satellites for high-precision position the buoy, for example , in the in-situ test region of the paper there are about 37 satellites can be adopted for the GNSS buoy about 25 satellites collected during the test, among which there are about 7 GPS satellites (Shan 2022). In its time system, Stellar Time, Solar Time, Universal Time, Atomic Time etc. are adopted, and every kind of satellites applied time system can be exchanged into a consistent time system, UTC. GNSS adopts its own relatively independent earth coordinate system, every satellite earth coordinate system is exchanged into it owns. GNSS basic observations mainly include pseudo-range observation, carrier phase observation, Doppler frequency shift observation, and carrier to noise ratio for position and velocity. In the GNSS, three displacements of the buoy are measured in vertical, north-south and east-west direction by PPP ionosphere free combination, and corresponding velocities are also measured in the three directions by Doppler frequency shift method which are independent on corresponding displacements. The measurement technique for wave observation is an advanced technology which adopts much more satellite to high-precision locate the buoy position and to measure its velocity with PDOP between 1.2 and 1.6 during the test and vertical velocity accuracy 2~3cm/s.

2.3 In-situ wave data observation

The GNSS wave buoy and a Waverider of DWR-G with diameter 0.4m are put on a sea surface to compare the wave observation data for evaluation the GNSS wave measurement technology (Fig.1). In the area, the water depth is 14m, wave height is around 1m, and wave period is about 4~5s. Two wave buoys are very closely deployed with the distance about 6m, so the wave data should be similar to each other. Detail technical indicators of the Waverider are listed in table 1. The Waverider adopts GPS based wave senser, with sampling frequency 1.28Hz. The GNSS wave buoy has a sampling frequency 5Hz. Wave profiles can be synchronous as shown in Fig.2. The time series of north-south, west-east and vertical displacements are measured by the Waverider buoy, while three displacements and corresponding velocities are measured by the GNSS buoy.

Fig.1 GNSS and wave buoy

Table.1 Technical indicators of the Waverider

Parameter	Value
Displacement in vertical, north and west direction	
Range	-20 m --- +20 m
Resolution	1 cm
Accuracy	±1 cm or 0.1% of value
Period	1.6 s --- 100 s
Wave direction	
Range	0^0 --- 360^0
Resolution	1.5^0
Accuracy	1.5^0
Reference	True north

3 Application of GNSS

3.1 Measurement Data

From 2019-10-29 6:00 to 2019-10-29 9:30, every 10 minutes wave data are recorded within eight half hours. Fig.2-1 shows the typical vertical displacements measured by Waverider and GNSS. The wave time history data are synchronous. At first glance, it seems that wave profiles have the same phase and fluctuate. In fact, most of crests and troughs are quiet difference. The crests of data by GNSS are slightly higher than that by Waverider, and the troughs of data by GNSS are slightly lower than that by Waverider. To be seen clearly, Fig.2-2 shows the typical enlarged figures from the first starting 100 seconds. More small fluctuation of the profiles by GNSS than that by Waverider. Lots of the difference are clear in the figure.. Detailed information can be compared by statistical analysis.
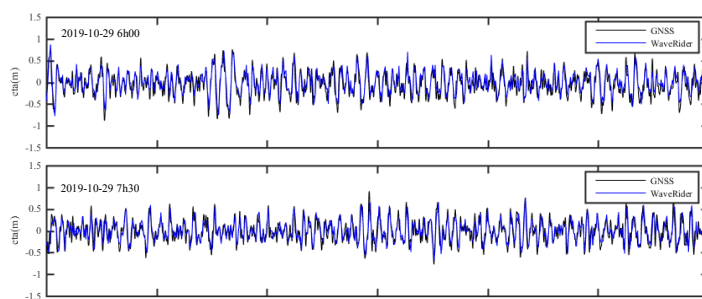

Fig. 2-1   Free surface elevation of GNSS and WaveRider within every 10 minutes
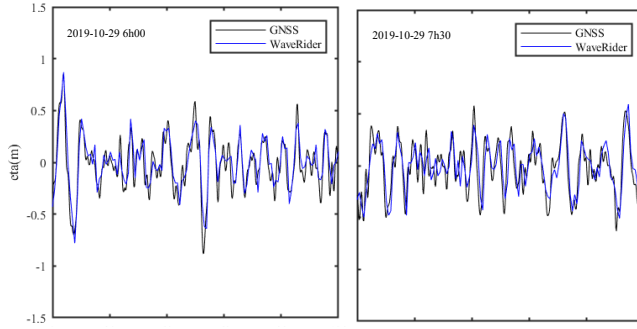
Fig.2-2 Free surface elevation of GNSS and WaveRider in details

3.2 Statistic analysis method

In wave buoy measurement system, vertical displacement is very important, which can be analyzed to supply wave height and period. Statistically, mean, standard deviation, skewness and kurtosis of a time history of displacement η_i are expressed as following formulas.

$$\bar{\eta} = \frac{\sum_{i=1}^{n} \eta_i}{n}, \quad \sigma = \sqrt{\frac{1}{n}\sum_{i=1}^{n}(\eta_i - \bar{\eta})^2}, \quad Sk = E\left[\left(\frac{\eta_i - \bar{\eta}}{\sigma}\right)^3\right], \quad Ku = E\left[\left(\frac{\eta_i - \bar{\eta}}{\sigma}\right)^4\right] \qquad (1)$$

Based on the above formulas, the statistical values of vertical displacement are calculated, which are listed in Table.2. It can be seen that by the two instruments eight half hour data have characteristics of that the means are tiny, the standard deviations are close, the skewness and kurtosis are quiet difference, and the skewness sometime has big difference, for example, at 2019-10-29 6:30 the difference value reaches 0.07 and -0.09 respectively for GNSS and Waverider. However, these two instruments are put in a very closed sea area, objectively the measured results should be very close, while measurements have some difference. Main reasons to the difference may be sampling frequency and buoy's shape. Influence by sampling frequency would be analyzed in the next section. If the shape or structure of GNSS buoy is optimal, it is not sure. Because that influence by Buoy's shape is very complicated, it will be studied in another paper.

Table.2   Statistic value of heave motion by GNSS and WaveRider

Start time	Mean (m)		Standard deviation (m)		Skewness		Kurtosis	
	GNSS	Waverider	GNSS	Waverider	GNSS	Waverider	GNSS	Waverider
6h00	0.00	0.00	0.27	0.26	0.02	0.01	3.05	2.95
6h30	0.00	0.00	0.28	0.27	0.07	-0.09	3.04	3.00
7h00	0.00	0.00	0.26	0.26	0.15	0.10	2.78	2.94
7h30	0.00	0.00	0.25	0.24	0.23	0.19	2.83	2.86
8h00	0.00	0.00	0.27	0.26	0.06	0.01	2.89	2.82
8h30	0.00	0.00	0.28	0.27	0.08	0.10	2.86	2.82
9h00	0.00	0.00	0.29	0.29	0.10	0.10	2.87	2.92
9h30	0.00	0.00	0.30	0.29	0.03	0.03	2.70	2.80

Wave height and period are analyzed by the up-zero method to the time history of vertical displacement. The characteristic wave height and period are statically calculated based on the vertical displacements of these two wave buoys.

3.3 Analyzed result

Based on the statical analyzing method, the maximum wave height H_{max}, the one-tenth wave height

$H_{1/10}$, the one-third wave height $H_{1/3}$, the mean wave height H_{ave}, and corresponding wave period as well as the number of waves are analyzed and listed in Table.3-1. The number of waves in each ten minutes by GNSS is greater than that by Waverider. The mean wave heights are very close, but other wave heights by GNSS are slightly greater than that by Waverider. The mean and one-third wave periods by GNSS are shorter than that by Waverider, while the wave period corresponding to H_{max} and the one-tenth wave period by GNSS sometimes longer or sometimes shorter. The reason is that the GNSS has higher sampling frequency, it may capture elaborate water free surface variation, which means that the GNSS has a relatively higher sensitivity than the Waverider. Measurement data of GNSS can be downsampled by sample frequency 1.25Hz, based on which wave characteristic are analyzed and listed in Table.3-2. Differences of the number of waves from the instruments decreased from about 30% larger than Waverider to less than about 10% after downsampled the GNSS data, wave height and wave period of these two instruments are closer than that without downsampling. Wave heights from GNSS are still slightly higher than that from Waverider, and wave periods from GNSS are still smaller than that from Waverider. By comparing the data between table 3-1 and 3-2, it is found that high sample frequency may presented smaller wave period, because that the GNSS sensor can capture small fluctuation of the water free surface. The analyzed data by that with or without downsample reflected high frequency sample present more accuracy result than downsample. Different wave heights (H_{max}, $H_{1/10}$, $H_{1/3}$ and H_{ave}) have their inherent feature of the ocean. Based on sampling frequency can reasonably capture wave characteristics, the averaged wave height is similar by different frequency sampling which reflected nature of waves.

Table.3-1   Statistic value of waves measured by GNSS and WaveRider

Start time	H_{max}	$H_{1/10}$	$H_{1/3}$	H_{ave}	$T(H_{max})$	$T_{1/10}$	$T_{1/3}$	T_{ave}	NW*
6h00	1.57/1.65**	1.29/1.18	0.99/0.92	0.60/0.61	10.20/7.81	8.25/8.17	6.59/7.39	4.38/5.38	136/111
6h30	1.80/1.41	1.32/1.22	1.05/0.99	0.64/0.65	7.80/8.59	6.71/7.50	6.56/7.08	4.43/5.56	134/107
7h00	1.41/1.45	1.16/1.20	0.95/0.94	0.58/0.59	7.60/8.59	8.15/7.95	6.65/7.48	4.38/5.22	136/114
7h30	1.39/1.2	1.14/1.05	0.92/0.86	0.56/0.56	4.6/7.03	6.51/7.17	6.37/6.83	4.23/5.19	141/114
8h00	1.60/1.47	1.24/1.16	0.97/0.99	0.60/0.65	6.80/7.03	7.06/7.58	6.40/7.25	4.33/5.60	138/105
8h30	1.54/1.41	1.28/1.17	1.05/0.98	0.63/0.65	8.20/8.59	7.08/7.81	6.56/6.79	4.38/5.47	136/108
9h00	1.68/1.54	1.34/1.26	1.09/1.06	0.68/0.68	8.20/9.38	7.88/7.67	6.60/7.12	4.57/5.38	130/111
9h30	1.57/1.48	1.37/1.30	1.12/1.07	0.72/0.70	6.20/5.47	6.31/6.68	6.30/6.80	4.35/5.28	137/113

Table.3-2   Statistic value of waves measured by GNSS downsampled and WaveRider

Start time	H_{max}	$H_{1/10}$	$H_{1/3}$	H_{ave}	$T(H_{max})$	$T_{1/10}$	$T_{1/3}$	T_{ave}	NW*
6h00	1.57/1.65**	1.24/1.18	0.95/0.92	0.61/0.61	10.4/7.81	9.02/8.17	7.16/7.39	5.10/5.38	116/111
6h30	1.76/1.41	1.28/1.22	1.03/0.99	0.66/0.65	8.00/8.59	7.42/7.50	6.93/7.08	5.02/5.56	118/107
7h00	1.36/1.45	1.14/1.20	0.93/0.94	0.60/0.59	7.20/8.59	8.51/7.95	7.16/7.48	4.97/5.22	119/114
7h30	1.35/1.2	1.10/1.05	0.91/0.86	0.59/0.56	8.00/7.03	6.91/7.17	6.83/6.83	5.01/5.19	119/114
8h00	1.49/1.47	1.21/1.16	1.00/0.99	0.65/0.65	7.20/7.03	6.98/7.58	6.97/7.25	5.19/5.60	114/105
8h30	1.44/1.41	1.23/1.17	1.05/0.98	0.68/0.65	8.00/8.59	7.27/7.81	7.24/6.79	5.33/5.47	110/108
9h00	1.62/1.54	1.33/1.26	1.07/1.06	0.70/0.68	8.00/9.38	8.22/7.67	6.81/7.12	5.03/5.38	117/111
9h30	1.56/1.48	1.37/1.30	1.13/1.07	0.75/0.70	5.60/5.47	6.47/6.68	6.26/6.80	4.93/5.28	121/113

Sample frequency: Waverider 1.28Hz, GNSS downsample to 1.25Hz

*The number of waves in every 10 minutes.

** a/b, a is obtained by GNSS, and b by WaveRider.

4 Wave spectrum analysis theory

4.1 Frequency spectrum

Theoretically, at a certain point the vertical displacement of a free wave surface can be assumed as that a frequency spectrum function is integrated from $-\infty$ to $+\infty$ in frequency domain.

$$\eta(t) = \int_{-\infty}^{+\infty} S(f)e^{i2\pi ft}df \tag{2}$$

Vice versa, the frequency spectrum is the time history of the vertical displacement integrated from $-\infty$ to $+\infty$ in temporal domain.

$$S(f) = \int_{-\infty}^{+\infty} \eta(t)e^{-i2\pi ft}dt \tag{3}$$

Discrete fast Fourier transform method is adopted to transfer the time history of the vertical displacement into frequency wave spectra. Both of data from GNSS and Waverider are analyzed for the eight half hours as shown in Fig.3. The frequency spectra distribution from GNSS and Waverider are consistent in each recorded time. Especially downsampled GNSS frequency spectra are closer than that of Waverider. Table.4 listed wave characteristics calculated by frequency spectra. The peak frequency of the eight times is about 0.11~0.14Hz, and the peak power density is 0.69~1.18 m^2/Hz. Significant wave height H_s and mean wave period T_{ave} are calculated by frequency spectra according to the following formula.

$$H_s = 4.0\sqrt{m_0}, \ T_{ave} = 2\pi\sqrt{m_0/m_2}, \ m_0 = \int_0^N S(f)df, \ m_2 = \int_0^N S(f)(2\pi f)^2 df \tag{4}$$

The significant wave height is in the range of 1.07~1.33m, and the mean wave period is 4.06~4.31s from GNSS, corresponding values from Waveriser are 1.03~1.20m and 4.77~5.07s and downsampled GNSS from 1.13~1.23m and 4.42~4.43s. Compared with statistical results, either the significant wave height from GNSS or from Waverider is slightly great, the statistical values are 0.92~1.12m of GNSS and 0.86~1.07m of Waverider, 0.91~1.13m of downsampled GNSS. While both the mean wave period calculated by spectra from GNSS and Waverider are smaller than that of statistical results, the statistical averaged wave periods are 4.23~4.57s of GNSS and 5.19~5.60s of Waverider, 4.93~5.33s of downsampled GNSS.
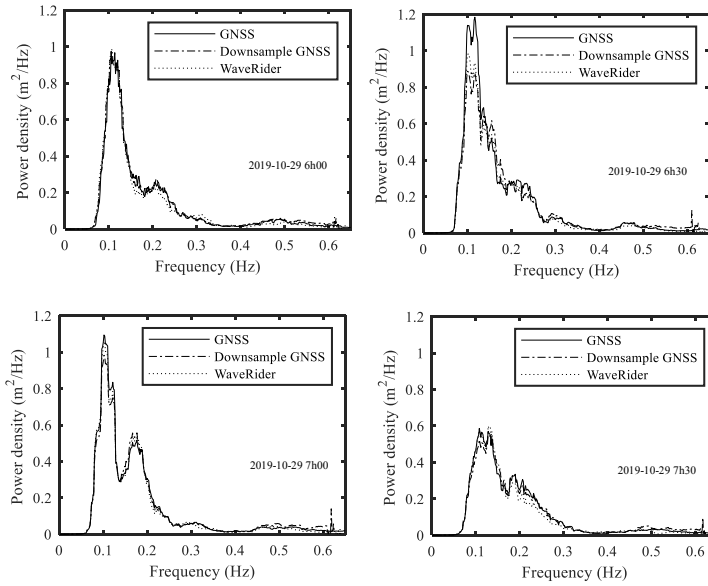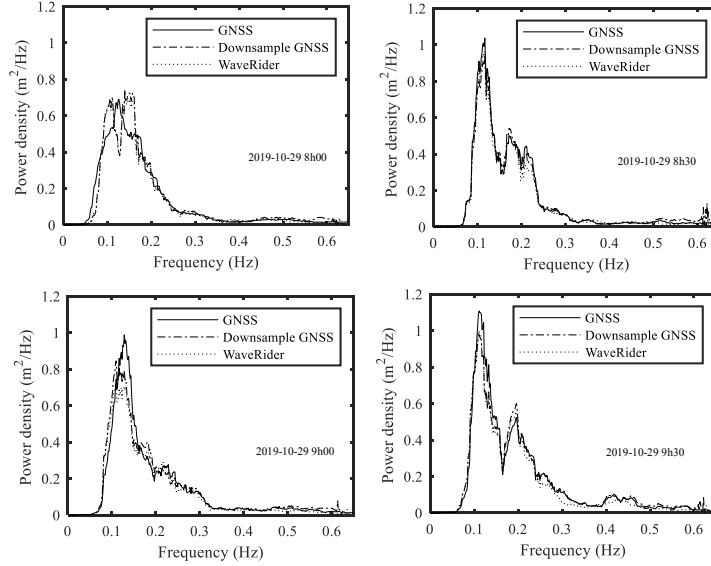
(Sample frequency : GNSS 5Hz, GNSS downsample to 1.25Hz, Waverider 1.28Hz； all data analyzed in ten minutes.)

Fig.3   Frequency wave spectrum by GNSS and WaveRider

Table.4   Wave characteristics by frequency wave spectrum

Start time	H_s	Tave (s)	f_p (Hz)	$S(f)_{max}$
2019-10-29 6h00	1.15/1.15/1.12*	4.15/4.43/4.85	0.11/0.11/0.11	0.97/0.97/0.99
2019-10-29 6h30	1.24/1.15/1.20	4.25/4.43/4.92	0.12/0.11/0.10	1.18/0.97/0.98
2019-10-29 7h00	1.19/1.15/1.17	4.22/4.42/4.96	0.11/0.11/0.10	1.02/0.97/1.06
2019-10-29 7h30	1.07/1.13/1.03	4.06/4.43/4.77	0.11/0.13/0.13	0.59/0.58/0.60
2019-10-29 8h00	1.16/1.15/1.17	4.31/4.43/5.02	0.13/0.11/0.14	0.69/0.71/0.70
2019-10-29 8h30	1.23/1.23/1.19	4.30/4.43/5.07	0.12/0.11/0.11	1.03/0.97/1.04
2019-10-29 9h00	1.22/1.15/1.17	4.18/4.43/5.02	0.13/0.11/0.13	0.99/0.96/0.90
2019-10-29 9h30	1.33/1.15/1.13	4.06/4.43/4.77	0.11/0.11/0.12	1.10/0.97/0.96

* a/b/c, a is obtained by that of GNSS with sample frequency 5Hz, b with GNSS downsample to 1.25Hz, and c by Waverider with sample frequency 1.28Hz.

4.2 Directional wave spectrum

Directional wave spectrum is thought as product of frequency spectrum and directional function.

$$S(f,\theta) = S(f)G(f,\theta) \tag{5}$$

The parametric directional wave spectrum is expressed as.

$$S(f,\theta) = S(f)[a_0(f) + \sum_n\{a_n(f)\cos(n\theta) + b_n(f)\sin(n\theta)\}] \tag{6}$$

where coefficient in the directional function $G(f,\theta)$ can be described by different manners. The GNSS buoy measured three displacements and velocities, in which velocities are independent of displacements in each direction, so that directional function can be built by three displacements or one displacement and two velocities, or three displacements and two velocities. However, Waverider only supplied displacements. In principle, the precision of directional function would be higher using more independent measured variables.

4.2.1 Directional function

The directional function $G(f,\theta)$ has three important properties, namely, wave energy conservation, positive in every direction and frequency.

$$\int_{-\pi}^{+\pi} G(f,\theta)d\theta=1, \ G(f,\theta) > 0 \tag{7}$$

Furthermore, the directional distribution of wave energy at any frequency has symmetric distribution, asymmetric distribution and multi-peak distribution.

4.2.1.1 Integrated area weight correction

In the manual of Waverider, the directional function is expressed as

$$G(f,\theta) = \frac{1}{\pi}\left[\frac{1}{2} + a_1\cos(\theta) + b_1\sin(\theta) + a_2\cos(2\theta) + b_2\sin(2\theta) + \cdots\right] \tag{8}$$

where the coefficients are obtained by the following procedure. In terms of the measured time series of displacements from north, west and vertical (n, w, v), three associated Fourier series can be calculated. Each Fourier series consists of a number of Fourier coefficients of real and imaginary part. The coefficients per frequency is express as $\alpha_{vf}, \alpha_{nf}, \alpha_{wf}, \beta_{vf}, \beta_{nf}, \beta_{wf}$, three vector series is noted

$$A_{vf} = \alpha_{vf} + i\beta_{vf}, A_{nf} = \alpha_{nf} + i\beta_{nf}, A_{wf} = \alpha_{wf} + i\beta_{wf} \tag{9}$$

Corresponding quadrature-spectra (C) and quad-spectra (Q) can be formed.

$$C_{nv} = \overline{A_{nf}} \bullet \overline{A_{vf}} = \alpha_{nf}\alpha_{vf} + \beta_{nf}\beta_{vf} \text{ and } Q_{nv} = \overline{A_{nf}} \times \overline{A_{vf}} = \alpha_{nf}\beta_{vf} - \beta_{nf}\alpha_{vf} \tag{10}$$

Finally, the coefficients in (8) are obtained.

$$a_1 = \frac{Q_{nv}}{\sqrt{(C_{nn}+C_{ww})\,C_{vv}}} \ , \ b_1 = \frac{-Q_{wv}}{\sqrt{(C_{nn}+C_{ww})\,C_{vv}}}, \quad a_2 = \frac{C_{nn}-C_{ww}}{C_{nn}+C_{ww}}, \ b_2 = \frac{-2C_{nw}}{C_{nn}+C_{ww}} \tag{11}$$

Based the above formula the directional function is calculated as shown in Fig.4 (a). Some direction of the directional function is negative. The negative value can be set to zero, an integrated area weight is introduced to keep it met Eqs. (7) the natural properties. Fig.4 (b) shows the corrected directional function.
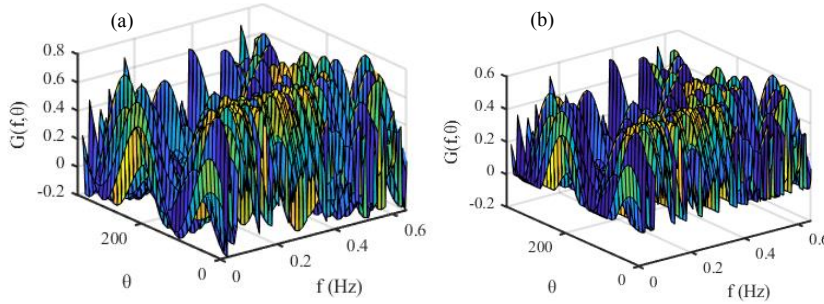

Fig.4 Directional function corrected by integrated area

An alternative expression of the directional function is introduced in the manual of Waverider.

$$G(f,\theta) = \frac{1}{\pi}\left[\frac{1}{2} + m_1\cos(\theta - \theta_0) + m_2\cos 2(\theta - \theta_0) + n_2\sin 2(\theta - \theta_0) + \cdots\right] \tag{12}$$

where

$$\theta_0 = \arctan(b_1, a_1), \ m_1=\sqrt{a_1^2 + b_1^2}, \ m_1=a_2\cos(2\theta_0) + b_2\sin(2\theta_0),$$
$$n_2=-a_2\sin(2\theta_0) + b_2\cos(2\theta_0) \tag{13}$$

Based on the formula, the directional function is calculated to the same three time series of displacement, which is very the same as shown in Fig.4.

4.2.1.2 Coefficient correction

In fact, researchers (Yu, 2003) have been designed correcting coefficient for Eqs. (8) and Eqs. (12). Applying these correcting coefficients, the directional function can be expressed as Eqs. (14) and Eqs. (15). By adopting Eqs. (14) and Eqs. (15), The same directional function can be obtained, which is shown in Fig.5, because that the results are calculated from the same Fourier coefficients.

$$G(f,\theta) = \frac{1}{\pi}\left[\frac{1}{2} + 2*(a_1\cos(\theta) + b_1\sin(\theta))/3 + (a_2\cos(2\theta) + b_2\sin(2\theta))/6 + \cdots\right] \quad (14)$$

$$G(f,\theta) = \frac{1}{\pi}\left[\frac{1}{2} + 2*m_1\cos(\theta - \theta_0)/3 + (m_2\cos2(\theta - \theta_0) + n_2\sin2(\theta - \theta_0))/6 + \cdots\right] \quad (15)$$
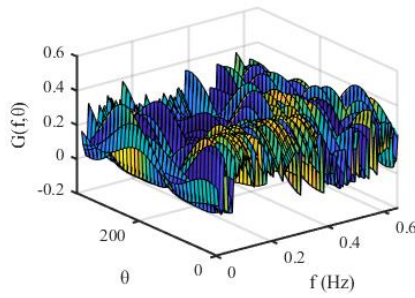

Fig.5 Directional function corrected by coefficient

4.2.1.3 $G(f,\theta)$ coefficients by displacement together with velocity

Similar to that in above $G(f,\theta)$ coefficients derivation from three displacements, they can be obtained from the time series of one displacement in heave direction and two velocities in north-south and west-east direction either. Corresponding six Fourier components are obtained as α_{1f}, α_{2f}, α_{3f}, β_{1f}, β_{2f}, β_{3f}, their vectors express as $A_{1f} = \alpha_{1f} + i\beta_{1f}$, $A_{2f} = \alpha_{2f} + i\beta_{2f}$, $A_{3f} = \alpha_{3f} + i\beta_{3f}$. Quadrature-spectra and quad-spectra are expressed as $C_{kl} = \overline{A_{kf}} \bullet \overline{A_{lf}} = \alpha_{kf}\alpha_{lf} + \beta_{kf}\beta_{lf}$ and $Q_{kl} = \overline{A_{kf}} \times \overline{A_{lf}} = \alpha_{kf}\beta_{lf} - \beta_{kf}\alpha_{lf}$, k, l=1,2,3. Then parameters for directional function are expressed as

$$p_1 = \frac{C_{12}}{\pi\sqrt{(C_{22}+C_{33})C_{11}}} , \quad q_1 = \frac{C_{13}}{\pi\sqrt{(C_{22}+C_{33})C_{11}}}, \quad p_2 = \frac{C_{22}-C_{33}}{\pi(C_{22}+C_{33})}, \quad q_2 = \frac{2C_{23}}{\pi(C_{22}+C_{33})} \quad (16)$$

The directional function adopted displacement in heave and velocities in in north-south and west-east direction is expressed as

$$G(f,\theta) = \frac{1}{\pi}\left[\frac{1}{2} + 2*(p_1\cos(\theta) + q_1\sin(\theta))/3 + (p_2\cos(2\theta) + q_2\sin(2\theta))/6 + \cdots\right] \quad (17).$$

It is also can be expressed by three displacements and two velocities as

$$G(f,\theta) = \frac{1}{\pi}\left[\frac{1}{2} + 4*(a_1\cos(\theta) + b_1\sin(\theta))/5 + 2*(a_2\cos(2\theta) + b_2\sin(2\theta))/5 + \cdots\right] +$$

$$\frac{1}{\pi}[4*(p_1\cos(\theta) + q_1\sin(\theta))/35 + (p_2\cos(2\theta) + q_2\sin(2\theta))/70 + \cdots] \quad (18).$$

Fig.6(a) and Fig.6(b) show the directional function obtained from Eqs. (17) and Eqs. (18) respectively. These two figures are quite different, while wave direction of each frequency is almost similar.
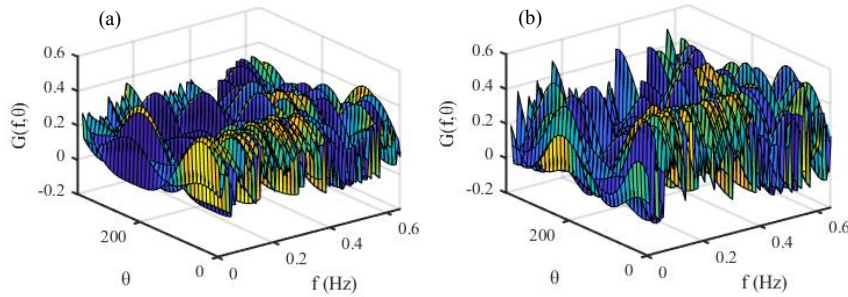
(a)

(b)

Fig.6 Directional function corrected by coefficient

4.2.2 Directional wave spectrum

4.2.2.1 Integrated area weight correction

Based on the measured three displacements at 2019-10-29 09:30, directional wave spectrum is calculated, the directional function is corrected by integrated area weight as above described. Fig.7 (a) is the directional wave spectrum in three-dimensional rectangular coordinate system, the peak spectrum function is around 45° with frequency around 0.1Hz, and the peak spectrum value is about 0.6 m^2/Hz. Fig.7 (b) is the directional wave spectrum in polar coordinate system, with contour express directional spectrum function. In the figure, there are two truncations in the range of 120° ~180° and 270° ~330°. From Fig.7, it seems the directional wave spectrum has two peaks, one big peak with direction about 45° and one small with direction about 225°.
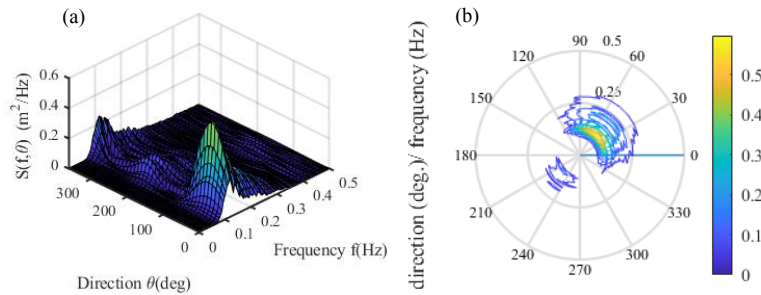

(a)

(b)

Fig.7 Directional wave spectrum by integrated area weight correction

4.2.2.2 Coefficient correction

Coefficients correction method applied to the direction function as formula (14), (17) and (18), the directional wave spectrum is calculated by measured data at 2019-10-29 09:00. Fig.8 (a) is calculated by formula (14) based on three displacements, it seems one peak in spectrum function with maximum close to 0.4 m^2/Hz, the peak direction is about 45°, and peak frequency about 0.1Hz. Fig.8 (b) calculated by formula (17) based on one heave displacement and two horizontal velocities. The direction spread angle is slightly large than that by formula (14), and the peak spectrum function slightly small. Fig.8 (c) calculated by formula (18) based on three displacements and two horizontal velocities. The peak spectrum function is greater than that of above two formulas, which reaches 0.5. The spread angle of wave direction slightly narrow, it is between 330°~150°. The peak directions by three formulas are almost

close, which are about 45º, while the last one may a little bit smaller than 45º. Comparison of the results is quite similar to common sense that more measured variables present high precision of directional function and directional spectrum.

(a)   Directional wave spectra by formula (14)

(b)   Directional wave spectra by formula (17)

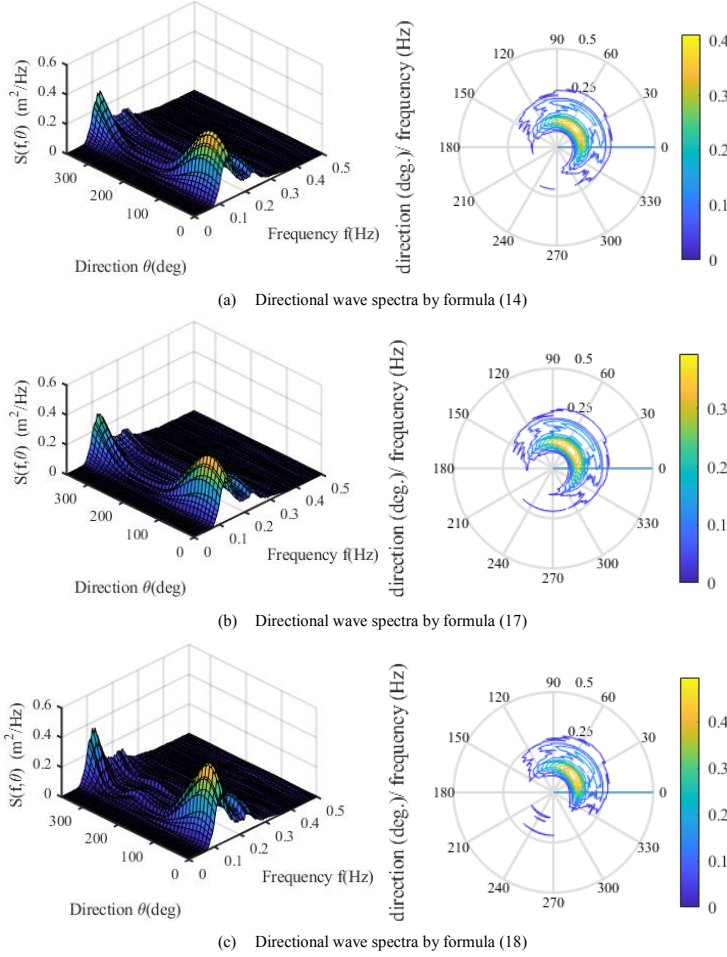(c)   Directional wave spectra by formula (18)

Fig.8 Directional wave spectrum corrected by coefficient

5 Results of directional wave spectrum

5.1 Characteristics of directional wave spectrum

The significant wave height and mean wave period can be calculated by directional wave spectrum as expressed in formula (4), when the m_0 and m_2 be calculated by directional wave spectrum. If the directional function is corrected by coefficients, the significant wave height and mean wave period are the same calculated by directional wave spectrum whether the directional function expressed by the formula (14), (15), (17) or (18). If the directional function is corrected by integrated area weight, the results have no difference either. Calculating results and statistical analyzing results from the measuring

data by GNSS are listed in Table.5. The significant wave height is in the range of 0.92~1.12m by statistical analysis, of 1.07~1.32m by directional wave spectrum using coefficients correction, and integrated aera weight correction. Based on the statistical results, the error is in the range of 12%~25% using coefficient correction, and integrated area weight correction. The mean wave period is in the range of 4.23~4.57s by statistical analysis, is of 4.06~4.31s using coefficient correction, and integrated aera weight correction. The error of the calculated mean wave period is less than 10%, and calculated values by directional wave spectrum are smaller than that by statistics. The calculated significant wave height and mean wave period are the same when wave spectrum corrected by coefficient and integrated area weight.

Table. 5 H_s and T_{ave} by Directional wave spectrum and statistical analysis

Start time	$H_{1/3}$	T_{ave}	Error of $H_{1/3}$ (%)	Error of T_{ave} (%)
2019-10-29 6h00	0.99/1.15/1.15*	4.38/4.15/4.15*	16/16**	-5.2/-5.2**
2019-10-29 6h30	1.05/1.24/1.24	4.43/4.25/4.25	18/18	-4.1/-4.1
2019-10-29 7h00	0.95/1.19/1.19	4.38/4.22/4.22	25/25	-3.7/-3.7
2019-10-29 7h30	0.92/1.07/1.07	4.23/4.06/4.06	16/16	-4.0/-4.0
2019-10-29 8h00	0.97/1.16/1.16	4.33/4.31/4.31	19/19	-0.5/-0.5
2019-10-29 8h30	1.05/1.23/1.23	4.38/4.31/4.31	17/17	-1.5/-1.5
2019-10-29 9h00	1.09/1.22/1.22	4.57/4.18/4.18	12/12	-8.5/-8.5
2019-10-29 9h30	1.12/1.32/1.32	4.35/4.06/4.06	17/17	-6.7/-6.7

* a/b/c, a is obtained by statistics, b by coefficient correction and c by integrated area weight correction.

** d/e, d is the value H_s or T_{ave} by coefficient correction minus $H_{1/3}$ or T_{ave} from statistics and divided by that from statistics, and e the value H_s or T_{ave} by integrated area weight correction minus $H_{1/3}$ or T_{ave} from statistics and divided by that from statistics.

5.2 Comparison of directional wave spectrum

In this part, in terms of eight times measuring data by GNSS and Waverider from 2019-10-29 6:00 to 2019-10-29 9:30, directional wave spectra are compared. Data by GNSS include time history of three displacements in vertical, north-south, west-east direction and two velocities in north-south, west-east direction. Data by Waverider include synchronous time-history of three displacements. Directional wave spectra are estimated based on the three displacements by formula (14) for data measured by GNSS and Waverider, and based on the three displacements and two velocities by formula (18) for data measured by GNSS. Fig.9 shows the directional wave spectra, in which the first two column is estimated by formula (14) and (18) for GNSS respectively, and the third column by formula (14) for Waverider. Based on directional wave spectrum, wave characteristics are listed in table.6.

From the in-situ measuring data, results can be compared in columns. When the directional wave spectra estimated by three displacements, it is shown that waves in-situ is changed not too large, the direction and spectra function are close. The two manners obtained directional wave spectra by GNSS present slightly different results. The wave direction of peak spectra is approximate, but the direction spread by formula (18) is less than that by formula (14), the difference is within 60°. Peak spectra function by formula (18) is larger than that formula (14), the difference is around 0.1 m²/Hz.

To compare the results obtained by GNSS and Waverider, the first column and the third column in the Fig. 9 are comparable, which are estimated by formula (14). Wave direction estimated by Waverider is spreading. Spread wave direction is almost larger than that by GNSS, the difference is in the range of 5°~40°. The peak spectra function are very close. Wave direction of peak spectra almost is approximate, that the difference is in the range of 2° ~10°.

In summary, the significant wave heights measured by GNSS are close to that by Waverider, while the mean wave periods by GNSS is 0.7s less than that by Waverider in case of wave period around 4~5s. The wave direction is concentrated when the directional wave spectra estimated by formula (18) for GNSS, in this case the peak spectra value is relatively large. It indicates that GNSS is a good instrument

for wave monitoring, especially by measuring three displacements and two velocities.

Table.6　Wave characteristics by Directional wave spectrum

| Start time	H_s	Tave (s)	f_p (Hz)	θ_p(deg.)	$S(f,\theta)_{max}$	S_p(deg.)*
2019-10-29 6h00	1.15/1.15/1.12*	4.15/4.15/4.85	0.11/0.11/0.12	28/18/34	0.40/0.50/0.39	105/90/142
2019-10-29 6h30	1.24/1.24/1.20	4.25/4.25/4.93	0.12/0.12/0.10	52/58/42	0.39/0.47/0.39	132/97/140
2019-10-29 7h00	1.19/1.19/1.17	4.22/4.22/4.96	0.11/0.11/0.10	32/32/26	0.41/0.55/0.41	122/88/135
2019-10-29 7h30	1.07/1.07/1.03	4.06/4.06/4.78	0.11/0.12/0.13	38/32/34	0.23/0.29/0.25	125/105/130
2019-10-29 8h00	1.16/1.16/1.17	4.31/4.31/5.02	0.13/0.12/0.12	38/32/34	0.28/0.35/0.34	130/100/135
2019-10-29 8h30	1.23/1.23/1.19	4.28/4.28/5.04	0.12/0.12/0.12	42/36/40	0.43/0.55/0.41	113/90/130
2019-10-29 9h00	1.22/1.22/1.17	4.18/4.18/5.02	0.13/0.13/0.12	44/36/44	0.41/0.50/0.38	120/105/132
2019-10-29 9h30	1.33/1.15/1.13	4.06/4.06/4.77	0.11/0.11/0.12	40/36/30	0.41/0.50/0.36	120/93/135

* S_p is the spread angle from the wave direction of the peak spectra.
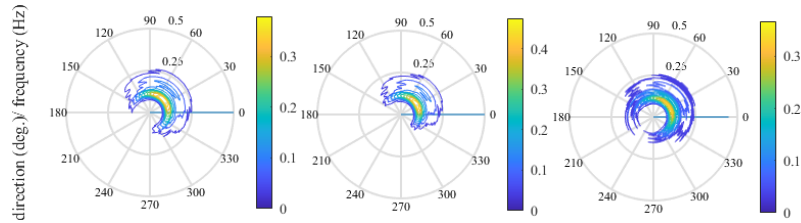
(d)　Directional wave spectra at 2019-10-29 6:00
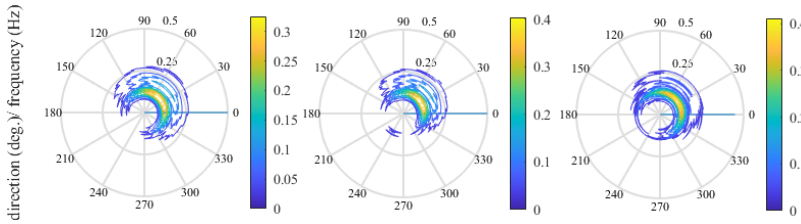
(e)　Directional wave spectra at 2019-10-29 7:30
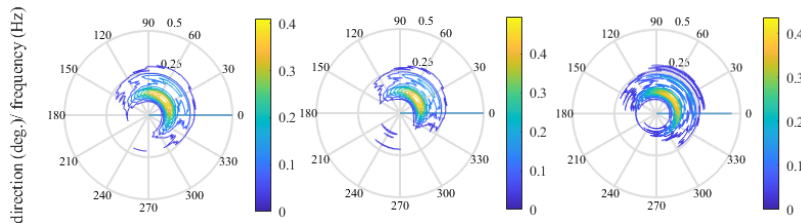
(f)　Directional wave spectra at 2019-10-29 9:00

Note: The first, second and third column are results by formula (14), (17) and (18) respectively.

Fig.9 Comparison of directional wave spectra by different method (to be continued)

6 Conclusion

To summarize, the GNSS wave buoy utilizes lots of satellites of which four global navigation satellite systems to implement high precision positioning and high precision Doppler velocity measuring for wave measurement, which has higher precision than adopting one navigation satellite system. In the paper, details of wave spectrum analysis method for the GNSS buoy are presented and wave data are compared

with that from Waverider to evaluate the GNSS measurement. Three displacements and two velocities can be synchronously measured using the GNSS buoy, which contributes the parametric directional wave spectra estimation with high concentration of wave direction and higher peaks of directional wave spectrum. It is found that mean wave height measured by GNSS buoy is very close to that by Waverider, while wave height $H_{1/10}$ and $H_{1/3}$ are slightly higher; mean wave period is about 15%~20% less by GNSS, from a statistical point of view. On the other hand, from spectrum analysis, significant wave height induced by wave spectrum is about 2%~4% higher by GNSS data than that by Waverider, and mean wave period is about 15% less by GNSS; peak frequency is very close by these two instruments; difference of wave direction at peak spectrum is within 16 degrees; difference of wave spread angle is in the range of 25~52, and GNSS data supply smaller one; value of peak directional spectrum is 25% higher by GNSS. When sample frequency of the GNSS is silimar to that of Waverider, errors of wave height are within 5%, and the differences of wave period are less than 0.5s. So the GNSS buoy can be used to measure wave data.

Reference

Antonov, V.S., Sadovskiy, I.N., 2007. Sea surface wave gauge IVMP-1: description of the device and measurement data of the fieldexperiment CAPMOS'05. *Roatprint IKI RAN*, Moscow

Ardhuin, F., Viroulet, S., Filipot, J.F., Benetazzo, A., Dulov,V., Fedele, F., 2010. Measurement of directional wave spectra using a wave acquisition stereo system: a pilot experiment. *Celebrating the 30th anniversary of the oceanographic platform in Kaciveli*.

Benoit, M., Frigaard, P., Schaffer, H.A., 1997. Analysing Multidirectional Wave Spectra: A tentative classification of available methods. *Iahr Congress*.

Bishop, C.T., Donelan, M.A. 1987. Measuring waves with pressure transducers. *Coast Eng*., 11, 309–328.

Borgman, L.E., 1969. Directional spectral model for design use for surface waves, *Hyd. End. Lab.*, Univ. Calif., Berkeley, HEL 1-12, 56.

Capon, J., 1969. High-resolution frequency-wave-number spectrum analysis. *Proc. IEEE*, 57, 1408-1418.

Datawell Waverider reference manual. 2010. Datawell BV Oceanographic instruments. July 28, 2010

Gendron, B.C., Chouaer, M.A., Santerre, R., Rondeau, M., & Seube, N., 2019. Wave measurements with a modified hydroball buoy using different gnss processing strategies. *Geomatica*.

Gorman, M.R., 2018. Estimation of directional spectra from wave buoys for model validation. *Procedia IUTAM*, 26, 81-91.

Gryazin. D. G., Gleb, K. A., 2022. A new method to determine directional spectrum of sea waves and its application to wave buoys. https://doi.org/10.1007/s40722-022-00228-z, *Journal of Ocean Engineering and Marine Energy*.

Gryazin, D.G., Gleb, K.A., 2019. The use of the stochastic control method in the study of the algorithm for calculating the characteristics of waves. *2019 III international conference on control in technical systems* (CTS) (October 2019), 1, Saint-Petersburg, Russia, 268–270.

Gryazin, D.G., Staroselcev, L.P., Belova, O.O., Gleb, K.A., 2017. Storm wave buoy equipped with micromechanical inertial unit: results of development and testing. *Oceanology*, 57(4), 605–610.

Hashimoto, N., 1997. Analysis of the directional wave spectrum from field data. *Adv. Coa. Ocean*

Eng., 3, 103-143, Philip L.-F. Liu, Editor

Hashimoto, N. and Kobune, K., 1985. Estimation of directional spectra from the Maximum Entropy Principle, *Rept. of P. H. R. I.* 23 (3), 123-145. (in Japanese)

Hasselmann, D.E., Dunckel, M. and Ewing, J.A., 1980. Directional wave spectra observed during JONSWAP, *J. Phys. Oceanogr.*,10, 1264-1280.

Hauser, D., Tison, C., Lefèvre J.M., Lambin, J., Thierry, A., Aouf, L., Collard, F, Castillan, P., 2010. Measuring ocean waves from space: objectives and characteristics of the China-France Oceanography SATellite (CFOSAT). *Proceedings of the international conference on offshore mechanics and arctic engineering*, 4, OMAE, Shanghai, China, 1–6.

Hauser, D., 2005. COST Action 714. Measuring and analysing the directional spectra of ocean waves. *Religious Education the Official Journal of the Religious Education Association*, 80-83.

Isobe, M. and Kondo, K., 1984. Method for estimating directional wave spectrum in incident and reflected wave field, *Proc. 19th ICCE*, Houston. 1, 467-483.

Lin, Y. P., Huang, C. J., & Chen, S. H., 2020. Variations in directional wave parameters obtained from data measured using a gnss buoy. *Ocean Engineering*, 209, 107513.

Longuet-Higgins, M.S., Cartwright, D.E., and Smith N.D., 1963. Observations of the directional spectrum of sea waves using the motions of a floating buoy. *Ocean Wave Spectra*, Prentice Hall, 111–136.

Mitsuyasu, H., Tasai, F., Suhara, T., Mizuno, S., & Rikiishi, K., 1975. Observation of the directional spectrum of ocean waves using a clover-leaf buoy. *Journal of Physical Oceanography*, 5(4).

Mitsuyasu, H., Tasai, F., Suhara, T., Mizuno, S., Ohkusu, M., Honda, T., and Rikiishi, K., 1975. Observations of the directional spectrum of ocean waves using a cloverleaf buoy. *J. Phys. Oceanogr*, 5, 750–760

Panicker, N.N. and Borgman L.E., 1974. Enhancement of directional wave spectrum estimate, *Proc. 14th ICCE*, Copenhagen. 258-279.

Purnell, D.J., Gomez, N., Minarik, W., Porter, D., and Langston, G., 2021. Precise water level measurements using low-cost GNSS antenna arrays. *Earth Surf. Dynam.*, 9, 673–685

Shan, R., 2022. Research on inversion method and application of wave and tide parameters based on GNSS technology. *Toji University，pHD thesis, August, 2022*

Shan, R., Cheng, X., Zhou, T., Cao, Y., Dong, L., 2019. Tide and Wave Measurement Based on High Precision Dynamic GNSS Technology. *The 40th Asian Conference on Remote Sensing* (ACRS 2019) October 14-18, 2019 / Daejeon Convention Center(DCC), Daejeon, Korea

Shan, R., Cheng, X., Yang, H., Lu, K. , Mei, S., Dong, L., 2018. Tide and Wave Measurement Application Researches Based on GNSS Technology. *20th EGU General Assembly*, EGU2018, Proceedings from the conference held 4-13 April, 2018 in Vienna, Austria, 3231

Smolov, V.E., Rozvadovskiy, A.F., 2020. Application of the Arduino Platform for Recording Wind Waves. *Morskoy Gidrofizicheskiy Zhurnal*, 36(4)

Sun, J., Burns, S., Vandemark, D., Donelan, M., Mahrt, L., Crawford, T., Herbers, T., Crescenti, G., French, J., 2005. Measurement of directional wave spectra using aircraft laser altimeters. J *Atmos Oceanic Tech*, 22, 869–885.

Wu, Z., 1994. Estimate approaches of η UV, PUV and UV directional wave spectra and their comparison. *The Ocean Engineering*, 12(4), 79-86. (in Chinese)

Wyatt, L.R., 2019. Measuring the ocean wave directional spectrum 'First Five' with HF radar. *Ocean Dyn*, 69, 123–144.

Yu, K., 2015. Tsunami-wave parameter estimation using gnss-based sea surface height measurement. *IEEE Transactions on Geoscience & Remote Sensing*, 53(5), 2603-2611.

Yu, Y., 2003. Random wave and its applications to engineering. *Dalian University of Technology Press*

Zhu, L., Yang, L., Xu, Y., Yang, F., & Zhou, X., 2020. Retrieving wave parameters from gnss buoy measurements using the ppp mode. *IEEE Geoscience and Remote Sensing Letters*, 99, 1-5.

Formatted: Font: Italic